Highly Sensitive GaN-WS$_2$-Based Surface Plasmon Resonance Sensor: a Theoretical Approach

Tanwin Mohammad Salauddin Ashrafi[1] · Goutam Mohanty[1]

Abstract

Utilizing an angular interrogation technique, the numerical design of a high-sensitivity surface plasmon resonance (SPR) structure is presented using a heterostructure GaN-WS$_2$, at an operational wavelength of He–Ne laser. The key performance parameters of the proposed sensor are computed and compared with other semiconductor and transition metal dichalcogenide (TMDC)-based SPR sensors. The investigation suggests that GaN has a significant impact on sensitivity. Furthermore, the inclusion of WS$_2$ layer on GaN resulted in a rise in sensitivity to levels comparable to graphene and other TMDC layers on it. Again, the evanescent electric field at the interface is significantly high for the proposed SPR structure. In addition, the values of detection accuracy (DA) and figure of merit (FOM) are superior in comparison to other GaN-TMDS-based SPR structures. The sensor construction with a heterostructure of 5 nm GaN and monolayer WS$_2$ coated on 55-nm silver results in a high sensitivity of 186.59(°/RIU), which is incredibly good in comparison to conventional SPR sensors and also, beneficial for the plasmonic research community.

Introduction

The plasmonic effect is caused by the interaction of free electrons in noble metal with incident polarized light. Surface plasmon resonance (SPR) exploits this effect to stimulate evanescent waves at the metal–dielectric interface using a TM-polarized wave at resonance [1, 2]. SPR applications are now vast in the fields of medical diagnostics, enzyme detection, drug diagnostics, and food safety [3–8]. Its popularity among sensing techniques stems from features such as high sensitivity, rapid response, and the ability to do real-time sensing on a label-free platform [9].

In 1968, Otto and Kretschmann produced an evanescent wave at the interface of two media at a particular angle due to the phenomena of attenuated total internal reflection (ATR) with polarized light [10, 11]. With a monochromatic light source, every variation in the refractive index of the sensing medium modifies the resonance angle to fulfill the resonance condition (angular interrogation method). The resonance condition is satisfied only if the wave vector of incident light and surface plasmon match each other [10, 11]. In the Kretschmann configuration, the metal coating is a key parameter. Noble metals are used for this purpose but each metal has merits and demerits. For high sensitivity, silver (Ag) is a potential candidate but less stable in comparison to gold (Au) [2, 9]. Many research groups are using graphene on the metal surface to protect it from oxidation and adsorb the hexagonal biological molecules in SPR sensors [12]. Also, Szunerits et al.reported that the graphene has many advantages which can be utilized to increase the sensitivity of SPR sensors [13]. Similarly, the use of high index semiconductor materials such as silicon (Si) increases the sensitivity of SPR sensor [14]. In addition to that, one of the authors of this manuscript reported that gallium nitride (GaN) on the metal surface is the superior choice in comparison to the Si-based SPR sensor [15] because GaN has a lot of superior properties such as non-toxic, high-temperature resistance, high chemical stability, and bio-friendly which helps to work in the harsh sensing environment [16].

In the last decades, research indicates that a family of exciting 2D materials, i.e., transition metal dichalcogenide (TMDC or TMD) such as tungsten diselenide (WSe$_2$),

✉ Goutam Mohanty
goutam.23352@lpu.co.in

1 Department of Physics, School of Chemical Engineering and Physical Sciences, Lovely Professional University, Phagwara, Punjab 144411, India

tungsten disulfide (WS$_2$), molybdenum diselenide (MoS$_2$), and molybdenum disulfide (MoSe$_2$) are useful in sensor applications due to their optical capabilities in SPR and localized surface plasmon (LSP) [17–21]. A few vital properties of TMDC over graphene are high adsorption rate, large tunable bandgap, and enormous bio-sensing work function. These properties attract the scientific community to explore the TMDC in plasmonic research. The authors believe that the combined heterostructres, i.e., semiconductor-TMDC or in more specifically GaN-TMDC in plasmonic research is a new concept and it is essential to study. In this study, an SPR-based sensor is explored using all the benefits of both GaN and TMDC materials.

Theory and Design Consideration

Based on the Kretschmann configuration, the proposed design is as follows: BK7 glass prism as the first layer, active metal (Ag) as the second layer, GaN as the third layer, 2D material as the fourth layer, and analytic as the fifth layer. He–Ne laser with wavelength 632.8 nm is used as TM polarized light as illustrated in Fig. 1.

In order to develop the proposed sensor, the first step is to optimize the thickness of all layers and then calculate the required performance parameters. For this purpose, the well-known transfer matrix method (TMM) has been used [15, 22, 23]. Using TMM, the key parameter, i.e., sensitivity (S) is calculated. The sensitivity is calculated by dividing the shifting in resonance angle ($\Delta\theta_R$) and change in refractive index (Δn_s) of the sensing medium due to adsorption of biomolecule and mathematically it can be written as $S = (\Delta\theta_R)$
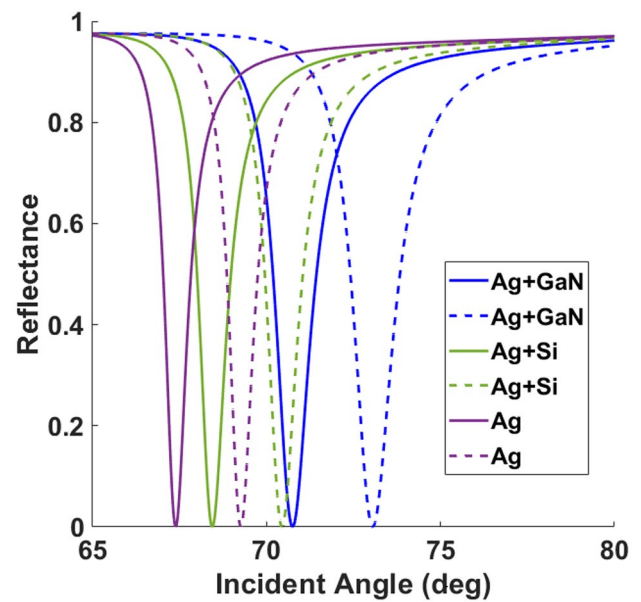
Fig. 2 SPR reflectivity curves for different SPR structures without TMDC

/ (Δn_s). Here the shift in resonance angle is $\theta_1 - \theta_2$, where θ_1 and θ_2 are the observed resonance angles at two different concentrations of sensing medium. θ_1 and θ_2 are calculated by looking at the corresponding minimum reflectance value in the SPR reflectivity curve. The reflectance value can be calculated using the following formula [15, 22, 23]:

$$R = \left| \frac{(W_{11} + W_{12}q_N)q_1 - (W_{21} + W_{22}q_N)}{(W_{11} + W_{12}q_N)q_1 + (W_{21} + W_{22}q_N)} \right|^2$$

where W_{ij} ($i, j = 1, 2$) is called characteristic matrix of the multilayer system and mathematically it can be written as,

$$W_{ij} = \left(\prod_{k=2}^{N-1} W_k \right)_{ij} ; i, j = 1, 2;$$

Table 1 The refractive indices of the materials

Materials	Refractive index	Reference
BK7	1.5151	[24]
Silver	0.056253 + 4.2760i	[25]
Gallium nitride	2.3848 + 0i	[26]
Silicon	3.8827 + 0.019626i	[27]
Graphene	3 + 1.149i	[28]
WSe$_2$	5.2302 + 0.50229i	[29]
WS$_2$	5.0646 + 0.23623i	[29]
MoS$_2$	4.9168 + 1.0554i	[29]
MoSe$_2$	5.2069 + 0.92551i	[29]
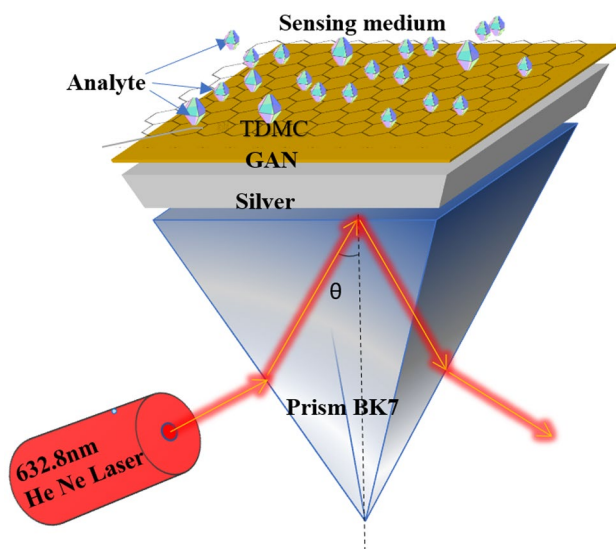
Fig. 1 Structure of the proposed sensor

Here, $W_k = \begin{pmatrix} \cos \xi_k & -i \sin \frac{\xi_k}{q_k} \\ -iq_k \sin \xi_k & \cos \xi_k \end{pmatrix}$; $q_k = \frac{(\varepsilon_k - n_1^2 \sin^2 \theta)^{1/2}}{\varepsilon_k}$;

and $\xi_k = d_k \left(\frac{2\pi}{\lambda}\right) \left(\varepsilon_k - n_1^2 \sin^2 \theta\right)^{1/2}$ where n_1 is the RI of first layer. d_k and ε_k are thickness and dielectric constant of kth layers respectively.

Subsequently, other parameters such as full width at half maxima (FWHM), detection accuracy (DA), figure of merit (FOM), and electric field enhancement have been computed. Mathematically, DA can be expressed as $(\Delta\theta_R)$ / FWHM

and FOM can be expressed as S / FWHM. For this study, the refractive indices (RI) of the materials at the wavelength 632.8 nm are tabulated in Table 1.

Results and Discussion

The performance parameters of the proposed SPR sensor are computed at 632.8-nm wavelength using TMM. First, the thickness of all layers is optimized by looking at the

Table 2 Resonance angle and sensitivity values of different SPR structures

| Structure	Thickness (m)	RI of sensing medium	Resonance angle (°)	Change in resonance angle (°)	Sensitivity (S) (°/RIU)
BK7-Ag-sensing medium	Ag = 55 nm	1.32919	67.39	ref	ref
		1.345	69.26	1.87	118.2796
BK7-Ag-semiconductor-sensing medium	Ag = 55 nm, Si = 1 nm	1.32919	68.44	ref	ref
		1.345	70.44	2	126.5022
	Ag = 55 nm, GaN = 5 nm	1.32919	70.75	ref	ref
		1.345	73.05	2.3	145.4775
BK7-Ag-2D layer-sensing medium	Ag = 55 nm, graphene = 0.34 nm	1.32919	67.64	ref	ref
		1.345	69.54	1.9	120.1771
	Ag = 55 nm, MoS$_2$ = 0.65 nm	1.32919	68.28	ref	ref
		1.345	70.26	1.98	125.2372
	Ag = 55 nm, MoSe$_2$ = 0.7 nm	1.32919	68.44	ref	ref
		1.345	70.45	2.01	127.1347
	Ag = 55 nm, WSe$_2$ = 0.7 nm	1.32919	68.46	ref	ref
		1.345	70.47	2.01	127.1347
	Ag = 55 nm, WS$_2$ = 0.8 nm	1.32919	68.58	ref	ref
		1.345	70.61	2.03	128.3997
BK7-Ag-Si-2D layer-sensing medium	Ag = 55 nm, Si = 1 nm, graphene = 0.34 nm	1.32919	68.73	ref	ref
		1.345	70.77	2.04	129.0323
	Ag = 55 nm, Si = 1 nm, MoS$_2$ = 0.65 nm	1.32919	69.53	ref	ref
		1.345	71.68	2.15	135.9899
	Ag = 55 nm, Si = 1 nm, MoSe$_2$ = 0.7 nm	1.32919	69.74	ref	ref
		1.345	71.93	2.19	138.5199
	Ag = 55 nm, Si = 1 nm, WSe$_2$ = 0.7 nm	1.32919	69.77	ref	ref
		1.345	71.96	2.19	138.5199
	Ag = 55 nm, Si = 1 nm, WS$_2$ = 0.8 nm	1.32919	69.91	ref	ref
		1.345	72.13	2.22	140.4175
BK7-Ag-GaN-2D layer-sensing medium	Ag = 55 nm, GaN = 5 nm, graphene = 0.34 nm	1.32919	71.14	ref	ref
		1.345	73.51	2.37	149.9051
	Ag = 55 nm, GaN = 5 nm, MoS$_2$ = 0.65 nm	1.32919	72.33	ref	ref
		1.345	74.9	2.57	162.5553
	Ag = 55 nm, GaN = 5 nm, MoSe$_2$ = 0.7 nm	1.32919	72.66	ref	ref
		1.345	75.3	2.64	166.9829
	Ag = 55 nm, GaN = 5 nm, WSe$_2$ = 0.7 nm	1.32919	72.71	ref	ref
		1.345	75.36	2.65	167.6154
	Ag = 55 nm, GaN = 5 nm, WS$_2$ = 0.8 nm	1.32919	74.12	ref	ref
		1.345	77.07	2.95	186.5908
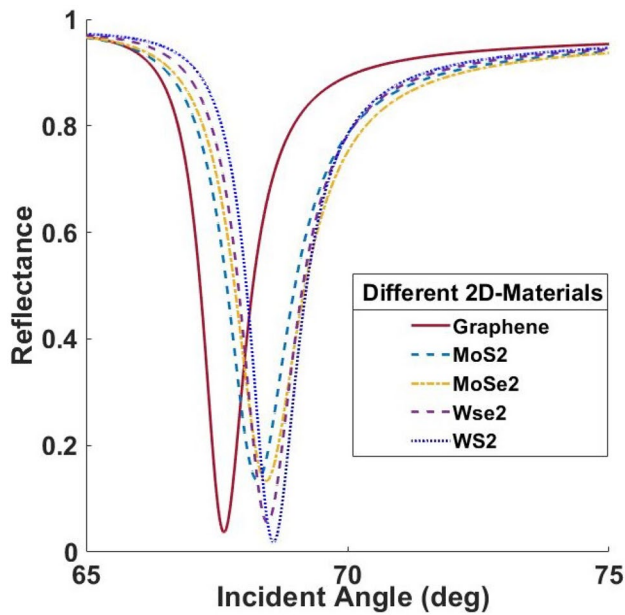
Fig. 3 SPR reflectivity curves for different SPR structures without semiconductor

minimum reflectance or plasmon dip with the help of the transfer matrix method (TMM). The optimized thickness of metal (Ag) is 55 nm. GaN optimal thickness has been found to be 6 nm for 1.32919 (RI of the sensing medium),
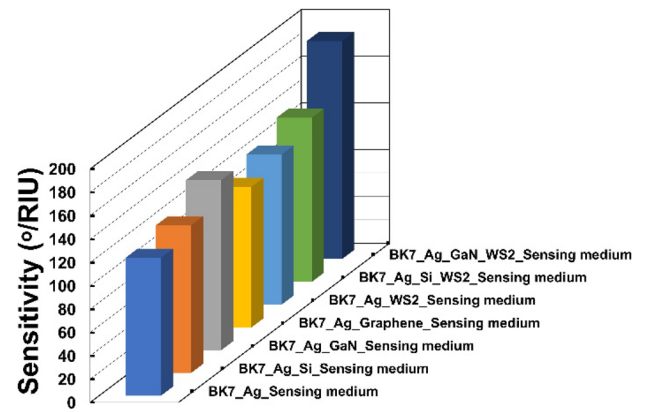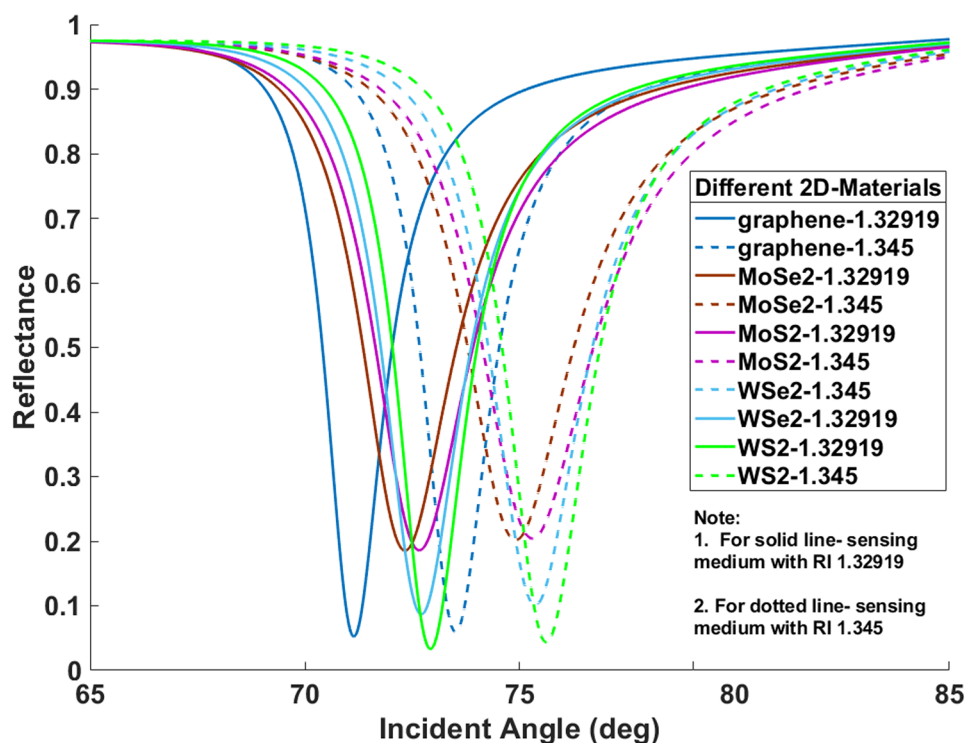

Fig. 5 Sensitivity values for different SPR structures

but as the refractive index of the sensing medium increases, the minimum reflectance value varies. For example, in the range of 1.32919 to 1.345, 5-nm thickness of GaN is the best choice for both the start and end of the range for the refractive index of the sensing medium. All the 2D layers such as graphene and TMDC materials are optimized and found with a minimum reflectance value for their monolayer thickness.

After optimization of all layers, the sensitivity of a particular SPR structure has been computed. Initially, the sensitivity values are computed by considering the SPR structure (i.e., BK7 glass-Ag-sensing medium and BK7

Fig. 4 SPR reflectivity curves for different SPR structures with 2D layer on GaN

Fig. 6 Sensitivity values for different SPR structures with 2D layer on GaN/Si
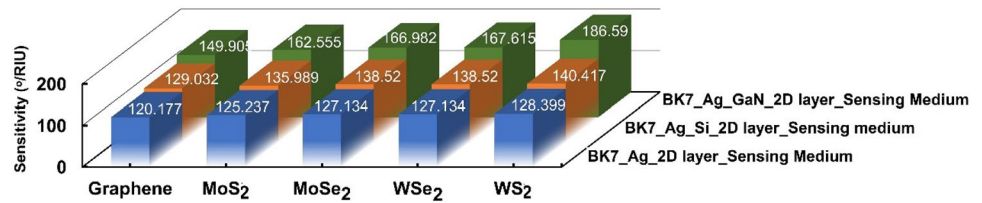
glass-Ag-semiconductor-sensing medium) without the TMDC layer. Figure 2 illustrates the SPR intensity curve for three- and four-layer systems. The essential point to consider from these observations is that GaN offers the largest increase in resonance angle with the rising refractive index of the sensing medium. The values of sensitivity for all structures without the TMDC layer are shown in Table 2. The unit of sensitivity is °/RIU (i.e., Degree per Refractive Index Unit).

Then the sensitivity values are computed by considering SPR structure (i.e., BK7 glass-Ag-2D material-sensing medium) without the semiconductor. Figure 3 presents a comparison of reflectance curves for several TMDC materials including graphene in SPR structure with a sensing medium having a RI of 1.32919. It is clearly indicated that the WS$_2$ heterostructure has shown the greatest drop, much exceeding graphene, and a maximum resonance angle. The

Fig. 7 Evanescent electric field at the interface of GaN-WS$_2$-based SPR structure

values of sensitivity for all structures without a semiconductor (GaN/ Si) layer are shown in Table 2.

In a similar way, the study has been extended by including both semiconductor and 2D layers in the SPR structure. Figure 4 shows the comparison SPR intensity curve for the GaN-2D material-based SPR structure in which the sensing medium RI ranges from 1.32919 to 1.345. The values of sensitivity for all structures with a semiconductor-TMDC layer are shown in Table 2.

Figure 5 shows the sensitivity variation with different layers SPR structure. In comparison to conventional SPR, the sensitivity remarkably improves with the introduction of semiconductors such as Si with a difference of 8.22 (°/RIU) and for GaN, it is 27 (°/RIU). When TMDC, such as WS$_2$, is used, sensitivity improves with a difference of 10.12 (°/RIU) from conventional SPR.

Figure 6 shows that the comparison 3D bar plot of sensitivity for different high index semiconductors and 2D layer-based SPR structure. The graph clearly shows the advantage of utilizing GaN, as it enhances sensitivity by 32.60%, while silicon only increases it by 8.64%. The effect of various 2D layers has also been explored, which gives sensitivity improvements of 1.60% with graphene, 5.89% with MoS$_2$, 7.5% with MoSe$_2$, 7.5% with WSe$_2$, and 8.55% with WS$_2$ when compared to the conventional SPR sensor. Thus, from Figs. 5 and 6, it is observed that the sensitivity of GaN-WS$_2$-based SPR structure is highest in comparison to other structures.

Again, 2D-simulation has been performed to analyze the evanescent electric field at the interface for all the above structures. The simulation is performed using electromagnetic wave frequency domain (ewfd) interface, wave optics modules in COMSOL Multiphysics. Figure 7 shows the surface plot of the evanescent electric field at the interface for GaN-WS$_2$-based SPR structure. Figure 8 shows the electric field enhancement results for different GaN-TMDC including graphene-based SPR structure. From Fig. 8, it is observed that the enhanced electric field for SPR structure with GaN-WS$_2$ optimized layers.

The values of detection accuracy (DA) and figure of merit (FOM) of all GaN-2D material-based SPR structures
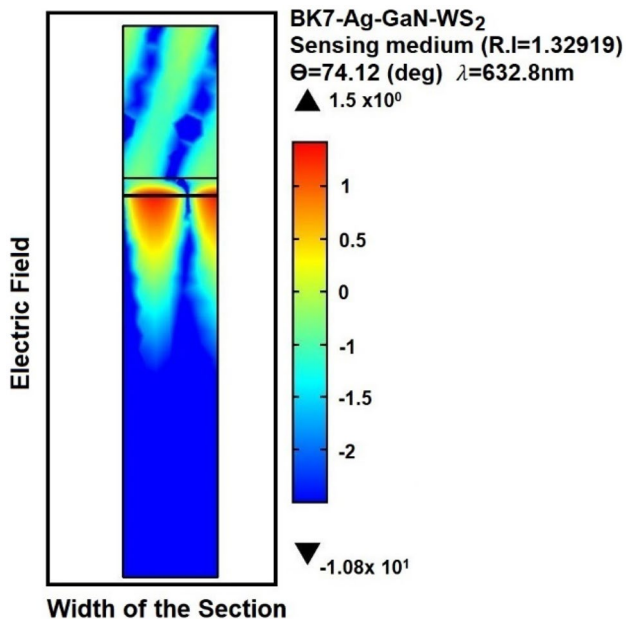
**Fig. 8** Evanescent electric field due to GaN-2D layer
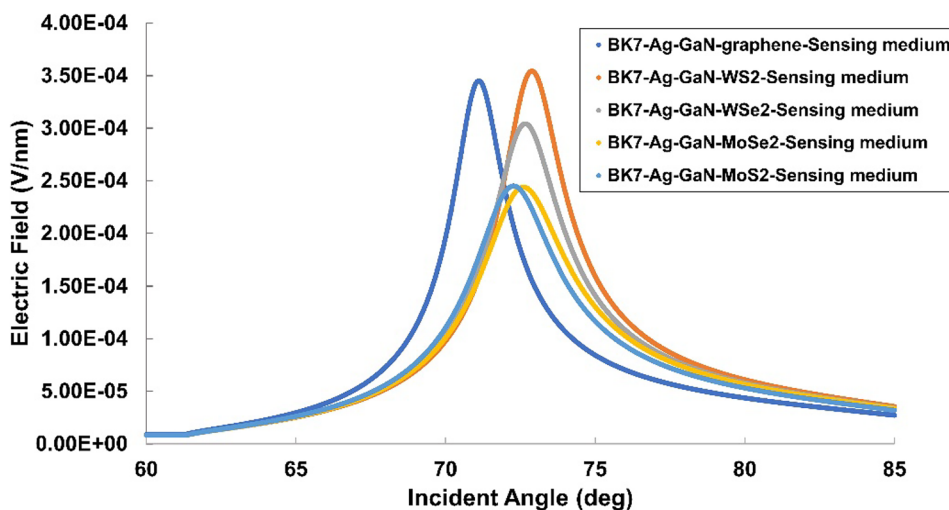
are computed and plotted below in Fig. 9 and Fig. 10 respectively. Figure 9 shows that DA of WS$_2$-based SPR structure gives superior value in comparison to other TMDC materials whereas graphene shows slightly higher value. Similarly, FOM of the WS$_2$-based SPR structure shows maximum value in comparison to other TMDC-based structures but little lesser than graphene (Fig. 10). In comparison with graphene, WS$_2$ is a good choice over graphene because it has many advantages such as protecting the underling metal layer from environmental corrosion, large surface to volume ratio, high adsorption rate, large tunable bandgap from visible to NIR spectrum, and

mammoth bio-sensing work function [30]. In addition to the above advantages, WS$_2$ consists of hexagonal crystal structure which makes it as a potential candidate for a wide variety of bio-sensing applications. A few research groups have already demonstrated that WS$_2$ is an efficient material for gas and humidity sensing applications [31, 32]. Hence, by considering all the above facts and observed performance parameters (i.e., high sensitivity, large electric field enhancement factor, and competitive values of DA and FOM), the heterostructure GaN-WS$_2$ provides a new pathway to develop a highly sensitive SPR sensor for various sensing applications.
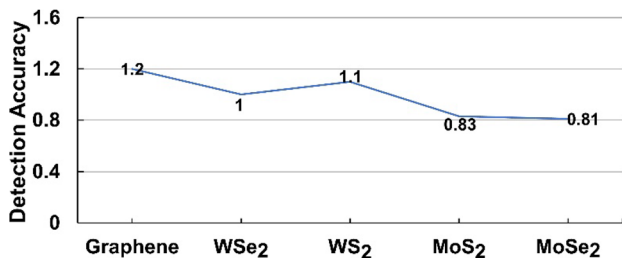
Fig. 9 DA values for GaN-2D layer-based SPR structures
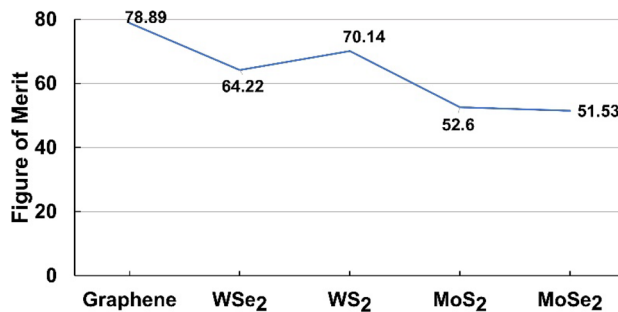
Fig. 10 FOM values for GaN-2D layer-based SPR structures

Conclusion

The overarching goal of SPR sensor research is to enhance sensitivity. As a result, the basic construction with an optimized layer of Ag will give sensitivity to a certain extent. In the present work, high index semiconductors such as GaN and silicon have been incorporated in to the conventional 3-layer SPR structure to achieve high sensitivity. To achieve further increased sensitivity, a few distinct types of monolayer TMDC and graphene is introduced on the surface of above semiconductor materials. The result shows that GaN and WS_2 are the best options to achieve the highly sensitive SPR sensor. Because the presence of GaN in SPR structure improves the sensitivity by 32.60% in comparison to silicon and the presence of WS_2 improves the sensitivity by 8.55% in comparison to all other TMDC layer. Again, the computed sensitivity of the GaN-WS_2-based SPR structure is 186.59 (°/RIU) which is the highest value in comparison to all other SPR structures. The electric field enhancement factor at the interface is observed highest for GaN-WS_2-based SPR structure. Also, the performance parameters such as DA and FOM of GaN-WS_2-based SPR structure are superior in comparison to other semiconductor-TMDC–based structures. From the above observations, the GaN-WS_2-based SPR structure is the best option to develop a high sensitivity SPR sensor for a wide variety of sensing applications.

Declarations

References

1. Maier SA (2007) Plasmonics: fundamentals and applications. Springer, New York
2. Homola J, Yee SS, Gauglitz G (1999) Surface plasmon resonance sensors. Sens Actuators B: Chem 54(1–2):3–15
3. Firdous S, Anwar S, Rafya R (2018) Development of surface plasmon resonance (SPR) biosensors for use in the diagnostics of malignant and infectious diseases. Laser Phys Lett 15(6):065602
4. Krishnamoorthy S (2015) Nanostructured sensors for biomedical applications - a current perspective. Curr Opin Biotechnol 34:118–124
5. Miyazaki CM et al (2017) Surface plasmon resonance biosensor for enzymatic detection of small analytes. Nanotechnology 28(14):145501
6. Su YW, Fang YM, Li TF (2021) Surface plasmon resonance sensing in cell biology and drug discovery. In Chen YP and Ma TF (ed) Comprehensive analytical chemistry. Elsevier, vol. 95, pp 1–53
7. Piliarik M, Párová L, Homola J (2009) High-throughput SPR sensor for food safety. Biosens Bioelectron 24(5):1399–1404
8. Situ C et al (2010) Advances in surface plasmon resonance biosensor technology towards high-throughput, food-safety analysis. Trends Anal Chem 29(11):1305–1315
9. Homola J (2003) Present and future of surface plasmon resonance biosensors. Anal Bioanal Chem 377(3):528–539
10. Kretschmann E, Heinz R (1968) Radiative decay of non radiative surface plasmons excited by light. Z für Naturforsch A 23(12):2135–2136
11. Otto A (1968) Excitation of nonradiative surface plasma waves in silver by the method of frustrated total reflection. Z Physik 216(4):398–410
12. Choi SH, Kim YL, Byun KM (2011) Graphene-on-silver substrates for sensitive surface plasmon resonance imaging biosensors. Opt Express 19(2):458–466
13. Szunerits S et al (2013) Recent advances in the development of graphene-based surface plasmon resonance (SPR) interfaces. Anal Bioanal Chem 405(5):1435–1443
14. Verma R, Gupta BD, Jha R (2011) Sensitivity enhancement of a surface plasmon resonance based biomolecules sensor using graphene and silicon layers. Sens Actuators B: Chem 160(1):623–631
15. Mohanty G, Akhtar J, Sahoo BK (2016) Effect of semiconductor on sensitivity of a graphene-based surface plasmon resonance biosensor. Plasmonics 11(1):189–196
16. Li X, Liu X (2017) Group III nitride nanomaterials for biosensing. Nanoscale 9(22):7320–7341
17. Zeng S et al (2015) Graphene-MoS2 hybrid nanostructures enhanced surface plasmon resonance biosensors. Sens Actuators B: Chem 207:801–810
18. Ouyang Q (2016) Sensitivity enhancement of transition metal dichalcogenides/silicon nanostructure-based surface plasmon resonance biosensor. Sci Rep 6(1):1–13
19. Mishra AK, Mishra SK, Verma RK (2016) Graphene and beyond graphene MoS2: a new window in surface- plasmon-resonance-based fiber optic sensing. J Phys Chem C 120(5):2893–2900
20. Wang H et al (2018) Sensitivity-enhanced surface plasmon resonance sensor utilizing a tungsten disulfide (WS_2) nanosheets overlayer. Photonics Res 6(6):485–491
21. Varasteanu P (2020) Transition metal dichalcogenides/gold-based surface plasmon resonance sensors: exploring the geometrical and material parameters. Plasmonics 15(1):243–253

22. Hansen WN (1968) Electric fields produced by the propagation of plane coherent electromagnetic radiation in a stratified medium. J Opt Soc Am 58(3):380–390

23. Born M (1964) Principles of optics: electromagnetic theory of propagation, interference and diffraction of light. Pergamon Press, Oxford

24. SCHOTT optical glass data sheets. http://refractiveindex.info. Accessed on 15 Jan 2022

25. Johnson PB, Christy RW (1972) Optical constants of the noble metals. Phys Rev B 6(12):4370

26. Barker AS Jr, Ilegems M (1973) Infrared lattice vibrations and free-electron dispersion in GaN. Phys Rev B 7(2):743

27. Aspnes DE, Studna AA (1983) Dielectric functions and optical parameters of Si, Ge, GaP, GaAs, GaSb, InP, InAs, and InSb from 1.5 to 6.0 ev. Phys Rev B 27(2):985

28. Bruna M, Borini S (2009) Optical constants of graphene layers in the visible range. Appl Phys Lett 94(3):031901

29. Hsu C et al (2019) Thickness-dependent refractive index of 1L, 2L, and 3L MoS_2, $MoSe_2$, WS_2, and WSe_2. Adv Opt Mater 7(13):1900239

30. Pawbake AS et al (2016) Highly transparent wafer-scale synthesis of crystalline WS2 nanoparticle thin film for photodetector and humidity-sensing applications. ACS Appl Mater Interfaces 8(5):3359–3365

31. Guan H et al (2017) Tungsten disulfide wrapped on micro fiber for enhanced humidity sensing. Opt Mater Express 7(5):1686–1696

32. O'Brien M et al (2014) Plasma assisted synthesis of WS_2 for gas sensing applications. Chem Phys Lett 615:6–10